

Cite this: *Chem. Sci.*, 2020, **11**, 11785

All publication charges for this article have been paid for by the Royal Society of Chemistry

# Combining alkali metals and zinc to harness heterometallic cooperativity in cyclic ester ring-opening polymerisation†

Weronika Gruszka,<sup>a</sup> Anna Lykkeberg,<sup>a</sup> Gary S. Nichol,<sup>a</sup> Michael P. Shaver,<sup>b</sup> Antoine Buchard<sup>c</sup> and Jennifer A. Garden<sup>\*a</sup>

Heterometallic cooperativity is an emerging strategy to elevate polymerisation catalyst performance. Here, we report the first heterotrimetallic Na/Zn<sub>2</sub> and K/Zn<sub>2</sub> complexes supported by a ProPhenol ligand, which deliver "best of both" in cyclic ester ring-opening polymerisation, combining the outstanding activity (Na/K) and good control (Zn<sub>2</sub>) of homometallic analogues. Detailed NMR studies and density-functional theory calculations suggest that the Na/Zn<sub>2</sub> and K/Zn<sub>2</sub> complexes retain their heterometallic structures in the solution-state. To the best of our knowledge, the K/Zn<sub>2</sub> analogue is the most active heterometallic catalyst reported for *rac*-lactide polymerisation ( $k_{\text{obs}} = 1.7 \times 10^{-2} \text{ s}^{-1}$ ), giving activities five times faster than the Na/Zn<sub>2</sub> complex. These versatile catalysts also display outstanding performance in  $\epsilon$ -caprolactone and  $\delta$ -valerolactone ring-opening polymerisation. These studies provide underpinning methodologies for future heterometallic polymerisation catalyst design, both in cyclic ester polymerisation and other ring-opening (co)polymerisation reactions.

Received 26th August 2020

Accepted 5th October 2020

DOI: 10.1039/d0sc04705h

rsc.li/chemical-science

## Introduction

Cyclic ester ring-opening polymerisation (ROP) is an efficient method for producing aliphatic polyesters such as poly(lactic acid) (PLA), poly( $\epsilon$ -caprolactone) (PCL) and poly( $\delta$ -valerolactone) (PVL).<sup>1–3</sup> The degradable and biocompatible properties of these polyesters have led to applications across packaging,<sup>4</sup> electronics and medicine.<sup>5</sup> ROP is dependent on the catalyst, and well-defined organometallic complexes have exerted excellent activities, selectivities and control over the polymer microstructure. The first examples comprised homoleptic homometallic alkoxides, *e.g.* Al(O<sup>*i*</sup>Pr)<sub>3</sub>, however bimetallic catalysts have recently gathered increased attention,<sup>6</sup> with most examples based on biocompatible Al, Ca, Fe, K, Na, Ti and Zn metals.<sup>7</sup> Despite the high activity of alkali metal catalysts,<sup>8</sup> bimetallic zinc catalysts are generally more efficient at combining high activities with polymerisation control in ROP.<sup>9–11</sup> We recently reported a highly active bimetallic zinc-benzoxide catalyst ([LZn<sub>2</sub>OBN]),<sup>12</sup> based on the Trost ProPhenol ligand (LH<sub>3</sub>), for the controlled homo- and co-

polymerisation of *rac*-lactide (*rac*-LA),  $\epsilon$ -caprolactone ( $\epsilon$ -CL) and *rac*- $\beta$ -butyrolactone.

The activity and selectivity of homometallic species can be enhanced by introducing a heterometal into the same complex, which can result in heterometallic cooperativity. Inspired by nature, which has long utilised heterometallic metalloenzymes in biological transformations,<sup>13,14</sup> chemists have observed unprecedented activity and selectivity enhancements with heterometallic complexes in metal-halogen exchange,<sup>15</sup> C–H bond activation<sup>16</sup> and olefin polymerisation.<sup>17,18</sup> However, the concept remains underexplored in cyclic ester ROP despite heterometallic complexes with a M–O–M' (M  $\neq$  M') framework (and thus intermetallic electronic communication *via* the O heteroatom) having the potential to enhance monomer coordination by increasing the metal Lewis acidity and accelerate propagation by enhancing the metal-alkoxide nucleophilicity.<sup>17,19</sup> To date, the best performing heterometallic catalysts for LA and  $\epsilon$ -CL ROP have generally comprised metals with large ionic radii and significant electronegativity differences between the metals, *e.g.* Al/Zn,<sup>20</sup> La/Mg,<sup>21</sup> Li/In,<sup>22</sup> Li/Mg and Li/Zn,<sup>23</sup> Li/Sm,<sup>24</sup> Na/Sm,<sup>25</sup> Sm/Al<sup>26</sup> and Ti/Zn<sup>27</sup> (Fig. 1). Combining Zn with electropositive alkali metals, which are highly active, inexpensive, earth abundant and non-toxic, is thus attractive from scientific, economic and environmental perspectives, yet remains underexplored.<sup>7</sup> Herein, the synthesis and activity of novel heterometallic complexes [LMZn<sub>2</sub>Et<sub>2</sub>(THF)<sub>2</sub>] (Fig. 1, where M = Na or K) are reported for cyclic ester ROP.

<sup>a</sup>EaStCHEM School of Chemistry, University of Edinburgh, Edinburgh, EH9 3FJ, UK. E-mail: j.garden@ed.ac.uk

<sup>b</sup>School of Natural Sciences, Department of Materials, Henry Royce Institute, University of Manchester, Manchester, M13 9PL, UK

<sup>c</sup>Department of Chemistry, University of Bath, Claverton Down, Bath, BA2 7AY, UK

† Electronic supplementary information (ESI) available: NMR, EA, MS characterisation data, polymer MALDI-ToF, GPC, kinetic and DOSY studies and DFT calculations. CCDC 2002496. For ESI and crystallographic data in CIF or other electronic format see DOI: 10.1039/d0sc04705h

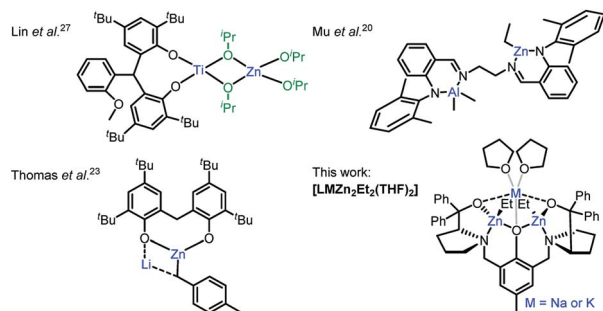


Fig. 1 Heterometallic M/Zn complexes reported for cyclic ester ROP.

## Results and discussion

### Homo- and hetero-metallic complex synthesis

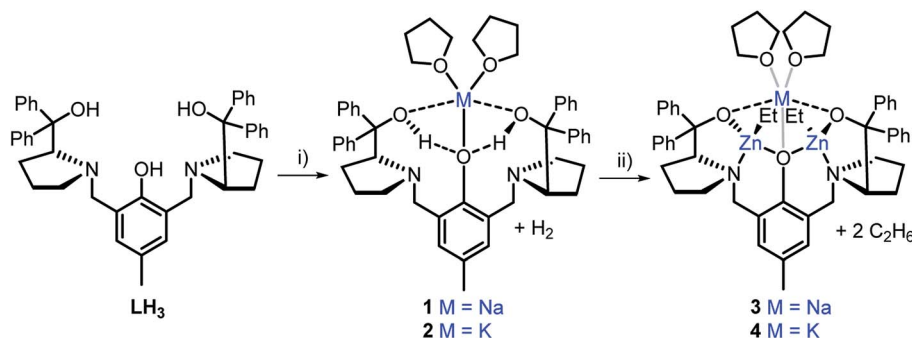
The heterometallic precursors  $[\text{LH}_2\text{Na}(\text{THF})_2]$  (**1**) and  $[\text{LH}_2\text{K}(\text{THF})_2]$  (**2**) were synthesised *via* mono-deprotonation of the phenolic-OH of  $\text{LH}_3$  with NaH or KH, respectively (Scheme 1), and characterised by NMR spectroscopy, mass spectrometry and elemental analysis (Fig. S1–S6†).  $^1\text{H}$  and DOSY NMR analysis indicated that **1** and **2** are centrosymmetric and mononuclear in THF- $d_8$  solution (Fig. S2 and S5†). Crystals of **1** were obtained by cooling a 1 : 1 THF : toluene mixture to  $-34^\circ\text{C}$ , yet despite multiple attempts, the crystals of **2** obtained were unsuitable for X-ray crystallographic analysis. **1** was mononuclear in the solid-state, with pentacoordinate Na displaying a low  $\tau$  value ( $\tau = 0.41$ , Fig. 2a)<sup>28</sup> suggesting that the structure is closer to a square pyramidal geometry than a trigonal bipyramidal geometry. The Na coordination sphere comprises a longer central Na1–O2 bond (2.355(5) Å) and four shorter dative bonds, two from the benzylic-OH [Na1–O1 (2.258(6) Å) and Na1–O3 (2.254(6) Å)] and two from THF [Na1–O4 (2.278(7) Å) and Na1–O5 (2.258(7) Å)]. In contrast to the solution-state, **1** was non-centrosymmetric in the solid-state, as evidenced by the tetragonal space group ( $P4_3$ ).

Although complex **1** features two benzylic OH groups that are acidified through hydrogen bonding to the phenolic O, these groups were not deprotonated with further equivalents of NaH ( $\leq 3$  eq. in total). This suggests that the product selectivity is influenced by both the  $\text{pK}_a$  of the OH groups and the ionic radii

of the alkali metals. Notably,  $\text{Na}^+$  and  $\text{K}^+$  are significantly larger (102 and 138 pm, respectively) than  $\text{Li}^+$  (76 pm),<sup>29</sup> and indeed, metalation of  $\text{LH}_3$  with  $n\text{BuLi}$  was less selective. NMR spectroscopic studies revealed two products, one symmetric (attributed to lithiation of the phenol-OH) and one asymmetric (lithiation of the benzylic OH). However, **1** and **2** were selectively deprotonated with 2 eq. of  $\text{ZnEt}_2$ , yielding complexes  $[\text{LNaZn}_2\text{Et}_2(\text{THF})_2]$  (**3**) and  $[\text{LKZn}_2\text{Et}_2(\text{THF})_2]$  (**4**) (Scheme 1), which were characterised by NMR spectroscopy, mass spectrometry and elemental analysis (Fig. S7–S12†). The centrosymmetric solution-state structure of **1** and **2** was also prominent in **3** and **4**, suggesting that each  $\text{Et}_2\text{Zn}$  deprotonates one benzylic OH and retains one ethyl group (Fig. S7 and S10†). DOSY NMR analysis suggests that **3** and **4** are both monomeric in the solution state (Fig. S8 and S11†). Unfortunately, attempts to isolate single crystals of **3** and **4** suitable for X-ray diffraction studies proved unsuccessful. However, density-functional theory (DFT) calculations confirmed the heterometallic structures and stability of **3** and **4** (refer to ESI†). The calculations suggest that the *R,R* configuration of the N atoms observed in the molecular structure of **1** is likely retained with **3'** and **4'** ( $'$  denotes computationally modelled structures, see ESI†), resulting in the two Zn–Et moieties facing in opposite directions relative to the phenol ring plane (Fig. 2b). However, ligand rearrangement to a *meso* (*R,S*) configuration at the N atoms, with Zn–Et groups facing in the same direction, was found to be only slightly endergonic for both **3'** (+2.0 kcal mol<sup>−1</sup>) and **4'** (+7.7 kcal mol<sup>−1</sup>) (Tables S6 and S13†).

### Rac-LA polymerisation: heterometallic vs. homometallic catalysis

Complexes **3** and **4** were found to be highly efficient initiators for *rac*-LA ROP with 2 eq. of benzyl alcohol (BnOH, Table 1). Complex **4** exhibited an exceptional polymerisation rate of  $k_{\text{obs}} = 1.7 \times 10^{-2} \text{ s}^{-1}$  in THF solvent at room temperature (R.T., Fig. S17†), converting 60 eq. of *rac*-LA in just 20 seconds. Not only is **4** five times faster than **3** ( $k_{\text{obs}} = 3.2 \times 10^{-3} \text{ s}^{-1}$ ) but it is, to the best of our knowledge, the most active heterometallic catalyst system reported for LA ROP and the first heterometallic K/Zn catalyst reported for cyclic ester ROP. Previously, some of the most active heterometallic catalysts for LA ROP were Li/Zn



Scheme 1 Synthesis of monometallic complexes **1** and **2** and heterometallic complexes **3** and **4**. Reagents and conditions: (i) 1.1 eq. MH, THF, R.T., 2 h; (ii) 2 eq.  $\text{ZnEt}_2$ , THF, R.T., 1 h.



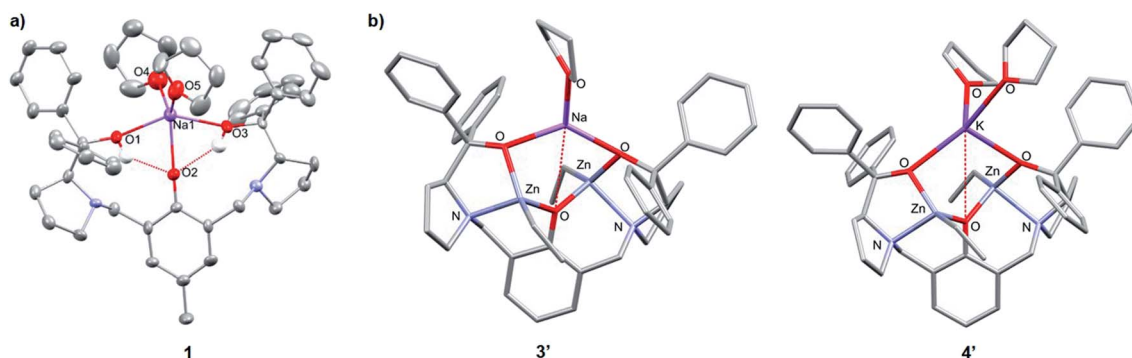


Fig. 2 (a) Molecular structure of **1**. Ellipsoids set at 50% probability level. H atoms and co-crystallised THF have been omitted for clarity. Selected bond lengths (Å): Na1–O1 2.258(6), Na1–O2 2.355(5), Na1–O3 2.254(6), Na1–O4 2.278 (7), Na1–O5 2.258(7). Selected bond angles (°): O1–Na1–O2 70.6(2), O2–Na1–O3 73.7(2), O1–Na1–O4 90.2(3), O3–Na1–O5 96.1(2), O4–Na1–O5 119.6(3). (b) Molecular structures of **3'** and **4'** with the lowest free enthalpies computed by DFT (refer to Tables S6 and S13†).

Table 1 ROP of *rac*-LA catalysed by complexes **1–4**, [BnONa], [BnOK] and [LZn<sub>2</sub>OBn]<sup>a</sup>

Entry	Cat.	Time (min)	Conv. <sup>b</sup> (%)	<i>M</i> <sub>n,obs</sub> <sup>c</sup> (Da)	<i>M</i> <sub>n,calc</sub> <sup>d</sup> (Da)	<i>D</i> <sup>e</sup>
1 <sup>e,f</sup>	<b>3</b>	2.5	12	—	—	—
2	<b>3</b>	0.33	47	2100	3400	1.3
3	<b>3</b>	2.5	71	3000	5100	1.2
4	<b>3</b>	7.5	86	3900	6200	1.4
5 <sup>e,f</sup>	<b>4</b>	2.5	13	—	—	—
6	<b>4</b>	0.08	45	1900	3300	1.7
7	<b>4</b>	0.33	60	2500	4300	1.4
8	<b>4</b>	1.25	81	3900	5800	1.4
9	<b>4</b>	2	93	4300	6700	1.4
10 <sup>e</sup>	<b>1</b>	1.25	79	14 800	11 400 <sup>g</sup>	4.1
11 <sup>e</sup>	[BnONa]	1.25	88	20 400	12 700 <sup>g</sup>	2.7
12 <sup>e</sup>	<b>2</b>	0.33	72	7300	10 400 <sup>g</sup>	4.3
13 <sup>e</sup>	[BnOK]	0.25	94	13 100	13 600 <sup>g</sup>	1.9
14 <sup>e</sup>	[LZn <sub>2</sub> OBn]	7.5	17	—	—	—
15 <sup>e,h</sup>	[BnOK] + [LZn <sub>2</sub> OBn]	0.25	99	8300	7100	1.6

<sup>a</sup> 100 : 1 : 2 LA : cat : BnOH, [LA] = 1 M in THF. <sup>b</sup> Calculated using <sup>1</sup>H NMR spectroscopy. <sup>c</sup> Determined by GPC using polystyrene standards in THF. Values corrected by Mark–Houwink factor (0.58).<sup>31</sup> <sup>d</sup> Calculated from the monomer conversion  $M_{n,calc} = M_0 \times ([M]/[I]) \times \text{conversion}$  assuming 2 chains per catalyst. <sup>e</sup> No BnOH used. <sup>f</sup> Polymerisations run at 60 °C. <sup>g</sup> Calculated from the monomer conversion  $M_{n,calc} = M_0 \times ([M]/[I]) \times \text{conversion}$  assuming 1 chain per catalyst. <sup>h</sup> [BnOK] generated *in situ* from KH and BnOH before adding [LZn<sub>2</sub>OBn].

and Li/Mg complexes supported by a bis(phenol) ligand,<sup>23</sup> which respectively converted 62 eq. and 88 eq. *rac*-LA in 15 min at R.T. in the presence of 1 eq. neopentyl alcohol. Complexes **3** and **4** (with 2 eq. of BnOH) also displayed activity for *rac*-LA ROP at 0.2–0.5 mol% catalyst loadings, generating PLA with *M*<sub>n</sub> of up to 12 100 g mol<sup>−1</sup> (Table S1†).

The polymerisations with **3** or **4** (and 2 eq. BnOH) were controlled with a linear relationship between *M*<sub>n</sub> and monomer conversion (Table 1, Fig. S18 and S19†). The discrepancy between the observed and calculated *M*<sub>n</sub> values was attributed to transesterification reactions, as evidenced by MALDI-ToF analysis

(refer to ESI†). End-group analysis revealed the expected  $\alpha$ -benzoy,  $\omega$ -hydroxy end-capped polymer chains. However, unlike related homometallic Trost ProPhenol catalysts ([**(LH)**<sub>2</sub>Zr]<sup>30</sup> and [LZn<sub>2</sub>OBn]<sup>12</sup>) no ligand end groups were detected with complexes **3** and **4**; this improved control may arise from the increased chelate stability and steric congestion of **3** and **4**. Similarly to homometallic [LZn<sub>2</sub>OBn],<sup>12</sup> the PLA generated from *rac*-LA was either atactic (maximum *P*<sub>i</sub> = 0.53 with **3**, Table S1†) or showed a modest isotactic bias (maximum *P*<sub>i</sub> = 0.62 with **4**). Kinetic studies of L-LA ROP (Fig. S34†) indicated that **4** is twice as active in *rac*-LA ROP (*k*<sub>obs</sub> = 1.7 × 10<sup>−2</sup> s<sup>−1</sup>) than L-LA ROP (*k*<sub>obs</sub> = 7.8 ×

$10^{-3} \text{ s}^{-1}$ ), whereas **3** displays similar polymerisation rates for *rac*- and *L*-LA ( $k_{\text{obs}} = 3.2 \times 10^{-3}$  and  $2.7 \times 10^{-3} \text{ s}^{-1}$ , respectively). These results suggest that while **3** likely has a similar degree of preference for *D*- and *L*-LA enchainment, **4** might display a slight preference for *D*-LA coordination and insertion, resulting in a modest isotactic bias. Notably, only trace *rac*-LA (<13%) was converted in the absence of BnOH co-initiator (Table 1, entries 1 and 5); these conversions were only mildly improved by the addition of 1 eq. BnOH to give 15% conversion with **3** after 5 min, and 20% conversion with **4** after 1.25 min (THF at R.T., Table S1,† entries 12 and 25). The dramatically reduced activity in the presence of 1 eq. BnOH suggests that **3** and **4** are unlikely to operate *via* an activated monomer mechanism as 2 eq. BnOH are required to efficiently initiate the proposed coordination-insertion mechanism. Complexes **3** and **4** also remained active under immortal polymerisation conditions (10 eq. BnOH, Table S1,† entries 13 and 26).

Complexes **3** and **4** were benchmarked against homometallic complexes **1–2**, [BnONa], [BnOK] and [LZn<sub>2</sub>OBn] in THF (Table 1). The alkali metal analogues were highly active but poorly controlled; the MALDI-ToF data shows transesterified  $\omega$ -hydroxy end-capped and cyclic PLA (see ESI†). [BnONa] and [BnOK] also displayed poor solubility in THF and toluene, emphasising a potential benefit of heterometallic initiators, which are often more soluble than the homometallic counterparts. Although [LZn<sub>2</sub>OBn] displays good activities in toluene,<sup>12</sup> the activity is diminished in THF (entry 14, Table 1). In contrast, **3** and **4** gave improved activities in THF, which was attributed to the Lewis acidic alkali metals, particularly the larger K<sup>+</sup> in **4** (vs. Na<sup>+</sup> in **3**), providing additional coordination sites, thus preventing competitive THF/LA coordination. Indeed, DFT calculations suggest a slight preference for coordination of 2 eq. THF to **4'** vs. 1 eq. THF to **3'** (Fig. 2, Tables S6 and S13†), even if coordination of 2 eq. THF to both **3** and **4** was observed by NMR analysis. Complexes **3** and **4** were also significantly faster than *in situ* generated [LZn<sub>2</sub>OBn] in *rac*-LA ROP in toluene at 60 °C (Table S3†), with **3** and **4** converting 89 eq. and 86 eq. *rac*-LA in 2.5 and 1 min, respectively (vs. 87 eq. in 10 min with *in situ* generated [LZn<sub>2</sub>OBn]). The activity and control differences between **3–4** and their homometallic analogues suggest cooperative interactions between Na/K and Zn<sub>2</sub>.

### Reactivity insights: experimental and computational studies

The *in situ* generation of [LNaZn<sub>2</sub>(OBn)<sub>2</sub>(THF)<sub>2</sub>] (**5**) and [LKZn<sub>2</sub>(OBn)<sub>2</sub>(THF)<sub>2</sub>] (**6**) from **3** or **4** and 2 eq. BnOH was investigated by NMR analysis in THF-*d*<sub>8</sub>, which indicated the rapid loss of BnOH and the formation of ethane (0.85 ppm) and new centrosymmetric complexes with OBn co-ligands (Fig. S44 and S45†). Notably, the Zn-Et groups of **3** remained intact in the presence of 10 eq. *rac*-LA until the addition of 2 eq. BnOH whereupon the Zn-Et groups disappeared and PLA was rapidly formed (Fig. S46†). DOSY NMR analysis of *in situ* generated **5** and **6** confirmed that the OBn co-ligands and **L** were part of the same complex (Fig. S47 and S48†). DFT calculations suggested **5'** and **6'** conserve the *R,R* ligand

stereochemistry at the N atoms (*vide supra*) but with ligand rearrangement to a *meso* (*R,S*) configuration also possible under the polymerisation conditions (Tables S9 and S14†). The *in situ* dissociation of **5** and **6** in THF to [LZn<sub>2</sub>OBn] and [BnONa] or [BnOK], respectively, was deemed unlikely based on NMR and DFT calculations (Fig. S49, S50 and Table S10†). The reaction of **1** and **2** with 1 eq. BnOH was also investigated but gave no reaction *i.e.* no [BnONa] or [BnOK] was formed (Fig. S51†). These findings suggest that the rearrangement of **3** and **4** to homometallic species is unlikely under the polymerisation conditions. This was further supported by monitoring the reaction of [LZn<sub>2</sub>OBn] with 1 eq. of *in situ* generated [BnOK] in THF-*d*<sub>8</sub> by <sup>1</sup>H NMR, which also generated **6** (Fig. S52†). Testing a 1 : 1 [BnOK] : [LZn<sub>2</sub>OBn] mixture in *rac*-LA ROP gave excellent activity in both THF and toluene (Tables 1 and S3†), albeit with reduced polymerisation control ( $\bar{D} = 1.6\text{--}2.0$ ) vs. [LZn<sub>2</sub>OBn] and **4** ( $\bar{D} < 1.5$ ). Similarly to LiCl addition boosting the activity of conventional Grignard reagents by forming heterometallic Turbo-Grignard reagents,<sup>32</sup> our findings suggest that addition of an alkali metal alkoxide to a bis-Zn complex may provide a simple yet effective strategy for improving the performance of homometallic ROP initiators. However, in this case, the optimal balance between the polymerisation activity and control was achieved with *in situ* generation of **5** and **6** *via* alcoholysis of **3** and **4** (Table 1, *vide infra*).

Coordination of 1–2 eq. *L*-LA to **5'** and **6'** was modelled by DFT (see ESI†); these reactions were either neutral or slightly exergonic. The most stable structures feature the *R,R* ligand configuration at the N atoms and one *L*-LA coordinated to the alkali metal, although coordination of two *L*-LA may also be accessible under polymerisation conditions. While no significant differences in structural and *L*-LA coordination preferences were found between **5'** and **6'**, the data suggests that coordination of two *L*-LA is more accessible for **6'** (vs. **5'**), in line with the increased ionic radius of K<sup>+</sup>. The activity differences between **3** and **4** (with 2 eq. BnOH) may thus have a kinetic origin; this requires modelling of ROP transition states which are currently under investigation in our laboratories.

Previous studies showed that isolated [LZn<sub>2</sub>OBn] gave a ten-fold activity increase vs. the *in situ* generated complex,<sup>12</sup> and so the isolation of **5** and **6** was investigated. However, the isolated heterometallic species showed reduced activity in *rac*-LA ROP compared to the *in situ* generated analogues (with 2 eq. BnOH); isolated **5** was approximately six times slower than **3**, and **6** gave half the rate of **4** (THF, R.T.). In contrast to *in situ* generated **5** and **6**, DOSY NMR analysis of isolated **5** and **6** (Fig. S54 and S55†) suggested formation of a two-component mixture involving higher MW species (approx. 826 Da in both cases) and lower MW species comprising OBn anions (252 Da for **5** and 298 Da for **6**). This may explain the reduced activity of the isolated species, as steric congestion around the metals in **5** and **6** could decrease the stability over time in THF (1 h at R.T.), leading to the formation of (mixed) metal-OBn aggregates. It is also plausible that increased concentration upon solvent removal for product isolation leads to formation of different





structures, as Lewis donor solvents are well-known to influence aggregation states of organometallic complexes. Importantly, on the timescale of the *in situ* generated polymerisations (<7.5 min at R.T. in THF), there was no evidence of decomposition by NMR analysis.

### Catalyst scope

Complex **3** (with 2 eq. BnOH) is also extremely active in  $\epsilon$ -CL and  $\delta$ -valerolactone ( $\delta$ -VL) ROP (Table S4<sup>†</sup>), converting 53 eq.  $\epsilon$ -CL and 99 eq.  $\delta$ -VL in just 5 s at R.T. Notably, **3** converts up to 760 eq.  $\epsilon$ -CL in 4 min at R.T., producing PCL with  $M_n$  up to 19 600 g mol<sup>-1</sup>. While complex **4** converted 94 eq.  $\delta$ -VL in 5 s, it was less active than **3** in  $\epsilon$ -CL ROP (Table S4<sup>†</sup>), which contrasts with the higher activity of **4** (vs. **3**) in *rac*-LA ROP. The more Lewis basic character of  $\epsilon$ -CL vs.  $\delta$ -VL and LA (based on the FT-IR carbonyl shifts:  $\nu(\text{C=O}) = 1732 \text{ cm}^{-1}$  for  $\epsilon$ -CL,  $1747 \text{ cm}^{-1}$  for  $\delta$ -VL and  $1770 \text{ cm}^{-1}$  for LA)<sup>33</sup> may promote decomposition/rearrangement of **4**; this may be more likely with **4** than **3** due to the larger and more electropositive K<sup>+</sup> centre facilitating  $\epsilon$ -CL coordination.

## Conclusions

In summary, two novel heterometallic complexes **3** and **4** were reported to be highly active in *rac*-LA,  $\epsilon$ -CL and  $\delta$ -VL ROP with 2 eq. BnOH. Complexes **3** and **4** outperform their homometallic counterparts, combining high activities with good polymerisation control. To the best of our knowledge, **4**/BnOH (2 eq.) is the fastest heterometallic catalytic system for *rac*-LA ROP reported to date. These rate enhancements demonstrate the benefit of combining metals known to be highly active in cyclic ester ROP (Zn) with abundant, inexpensive and non-toxic alkali metals (Na and K). When bridged through a heteroatom, electronic communication between heterometals can alter the properties of each metal through an "ate" activation. While alkali metals are known to boost the reactivity of Zn towards C–H activation,<sup>34</sup> our studies suggest that this concept can also be translated to cyclic ester ROP. The activity enhancements observed may arise from increased Lewis acidity of the more electropositive metal (Na/K) and labilisation of the M–OR bonds around the more electrophilic metal(s) (Zn). Heterometallic catalysts remain underexplored in ROP and offer a promising area for further investigation.

## Conflicts of interest

There are no conflicts to declare.

## Acknowledgements

We would like to thank the CRICAT Centre for Doctoral Training and EPSRC (W. G., EP/L016419/1; M. P. S.; EP/S025200/1 and EP/P026095/2), Royal Society (J. A. G., RSG/R1/180101; A. B., UF160021 fellowship), British Ramsay Memorial Trust (J. A. G.) and L'Oréal-UNESCO For Women in

Science (J. A. G.) for funding. We thank the University of Bath HPC for computing resources.

## Notes and references

- 1 M. J. Stanford and A. P. Dove, *Chem. Soc. Rev.*, 2010, **39**, 486–494.
- 2 C. K. Williams, *Chem. Soc. Rev.*, 2007, **36**, 1573–1580.
- 3 C. M. Thomas, *Chem. Soc. Rev.*, 2010, **39**, 165–173.
- 4 R. Auras, B. Harte and S. Selke, *Macromol. Biosci.*, 2004, **4**, 835–864.
- 5 C. Ha and J. A. Gardella, *Chem. Rev.*, 2005, **105**, 4205–4232.
- 6 A. B. Kremer and P. Mehrkhodavandi, *Coord. Chem. Rev.*, 2019, **380**, 35–57.
- 7 R. Platel, L. Hodgson and C. K. Williams, *Polym. Rev.*, 2008, **48**, 11–63.
- 8 J. Gao, D. Zhu, W. Zhang, G. A. Solan, Y. Ma and W.-H. Sun, *Inorg. Chem. Front.*, 2019, **6**, 2619–2652.
- 9 B. M. Chamberlain, M. Cheng, D. R. Moore, T. M. Ovitt, E. B. Lobkovsky and G. W. Coates, *J. Am. Chem. Soc.*, 2001, **123**, 3229–3238.
- 10 C. K. Williams, L. E. Breyfogle, S. K. Choi, W. Nam, V. G. Young, M. A. Hillmyer and W. B. Tolman, *J. Am. Chem. Soc.*, 2003, **125**, 11350–11359.
- 11 A. Thevenon, C. Romain, M. S. Bennington, A. J. P. White, H. J. Davidson, S. Brooker and C. K. Williams, *Angew. Chem., Int. Ed.*, 2016, **55**, 8680–8685.
- 12 W. Gruszka, L. C. Walker, M. P. Shaver and J. A. Garden, *Macromolecules*, 2020, **53**, 4294–4302.
- 13 K. C. MacLeod and P. L. Holland, *Nat. Chem.*, 2013, **5**, 559–565.
- 14 C. Wombwell and E. Reisner, *Dalton Trans.*, 2014, **43**, 4483–4493.
- 15 T. D. Bluemke, W. Clegg, P. Garcia-Alvarez, A. R. Kennedy, K. Koszinowski, M. D. McCall, L. Russo and E. Hevia, *Chem. Sci.*, 2014, **5**, 3552–3562.
- 16 A. J. Martinez-Martinez, A. R. Kennedy, R. E. Mulvey and C. T. O'Hara, *Science*, 2014, **346**, 834–837.
- 17 S. K. Mandal and H. Roesky, *Inorg. Chem.*, 2007, **46**, 10158–10167.
- 18 J. P. Mcinnis, M. Delferro and T. J. Marks, *Acc. Chem. Res.*, 2014, **13**, 2545–2557.
- 19 Z. Cai and D. Xiao, *Comments Inorg. Chem.*, 2019, **39**, 27–50.
- 20 A. H. Gao, W. Yao, Y. Mu, W. Gao, M.-T. Sun and Q. Su, *Polyhedron*, 2009, **28**, 2605–2610.
- 21 L. F. Sánchez-Barba, D. L. Hughes, S. M. Humphrey and M. Bochmann, *Organometallics*, 2006, **25**, 1012–1020.
- 22 M. Normand, E. Kirillov, T. Roisnel and J.-F. Carpentier, *Organometallics*, 2012, **31**, 1448–1457.
- 23 J. Char, E. Brule, P. C. Gros, M.-N. Rager, V. Guérineau and C. M. Thomas, *J. Organomet. Chem.*, 2015, **796**, 47–52.
- 24 W. Li, Z. Zhang, Y. Yao, Y. Zhang and Q. Shen, *Organometallics*, 2012, **31**, 3499–3511.
- 25 H. T. Sheng, J. M. Li, Y. Zhang, Y. M. Yao and Q. Shen, *Polyhedron*, 2008, **27**, 1665–1672.
- 26 J. Hao, J. Li, C. Cui and H. W. Roesky, *Inorg. Chem.*, 2011, **50**, 7453–7459.



- 27 H.-Y. Chen, M.-Y. Liu, A. K. Sutar and C.-C. Lin, *Inorg. Chem.*, 2010, **49**, 665–674.
- 28 A. W. Addison, T. N. Rao, J. Reedijk, J. Van Rijn and G. C. Verschoor, *J. Chem. Soc., Dalton Trans.*, 1984, 1349–1356.
- 29 R. D. Shannon, *Acta Crystallogr.*, 1976, **32**, 751–767.
- 30 B. Rajashekhar, S. K. Roymuhury, D. Chakraborty and V. Ramkumar, *Dalton Trans.*, 2015, **44**, 16280–16293.
- 31 A. Kowalski, A. Duda and S. Penczek, *Macromolecules*, 1998, **31**, 2114–2122.
- 32 A. Krasovskiy and P. Knochel, *Angew. Chem., Int. Ed.*, 2004, **43**, 3333–3336.
- 33 P. Dubois, C. Jacobs, R. Jerome and P. Teyssie, *Macromolecules*, 1991, **24**, 2266–2270.
- 34 R. E. Mulvey, *Acc. Chem. Res.*, 2009, **42**, 743–755.

